A Fast Calculation Method for Long-term Security-constrained Unit Commitment of Large-scale Power Systems with Renewable Energy

Qian Yang, Jianxue Wang, Hongrui Yin, and Qingtao Li

***Abstract*—With the increase in the penetration rate of renewable energy, the planning and operation of power systems will face huge challenges. To ensure the sufficient utilization of renewable energy, the reasonable arrangement for the long-term power generation plan has become more crucial. Security-constrained unit commitment (SCUC) is a critical technical means to optimize the long-term power generation plan. However, the plentiful power sources and the complex grid structure in large-scale power systems will bring great difficulties to long-term SCUC. In this paper, we propose a fast calculation method for long-term SCUC of large-scale power systems with renewable energy. First, a method for unit status reduction based on temporal decomposition is proposed, which will reduce plenty of binary variables and intertemporal constraints in SCUC. Then, an efficient redundant constraint identification (RCI) method is developed to reduce the number of network constraints. Furthermore, a joint accelerated calculation framework for status reduction and RCI is formed, which can reduce the complexity of long-term SCUC while ensuring a high-precision feasible solution. In case studies, numerical results based on two test systems ROTS2017 and NREL-118 are analyzed, which verify the effectiveness and scalability of the proposed calculation method.**

***Index Terms*—Accelerated calculation framework, long-term security-constrained unit commitment (SCUC), redundant constraints identification, renewable energy, unit status reduction.**

NOMENCLATURE

A. Sets

Ω_D	Set of loads
Ω_G	Set of conventional units
Ω_L	Set of transmission lines
Ω_P	Set of conventional power plants
$\Omega_{P,i}$	Set of conventional units in power plant i
Ω_R	Set of renewable energy units
Ω_T	Set of time periods

B. Parameters

α^{RS}	Reserve factor
β^R	Power curtailment cost of renewable energy units
σ^P	The maximum deviation between the actual power generation and contracted power generation of conventional power plants, which is 5% in this paper
$\boldsymbol{\Gamma}_t$	$2NL$ dimensional vector at time t
$\gamma_{j,t}$	The j^{th} row element of $\boldsymbol{\Gamma}_t$
Δt	Time granularity, which is 1 hour in this paper
$C_i(\cdot)$	Generation cost function of conventional unit i
D_t	Load demand of the whole power system at time t
$f_{j,v_m}^{U'}$	Element in the j^{th} row and v_m^{th} column of matrix $\boldsymbol{F}^{U'}$
$F_{l,i}^G$, $F_{l,i}^R$, $F_{l,i}^D$	Distribution factors of conventional unit i, renewable energy unit i, and load i to line l
$F_{l,i}^U$	Distribution factor of unit i to line l
$\boldsymbol{F}^U$	$2NL \times NU$ dimensional matrix
$h_{i,j}$	Slope of segment j of linearized $C_i(\cdot)$
$k_{i,j}$	Intercept of segment j of linearized $C_i(\cdot)$
n	Number of segments of linearized $C_i(\cdot)$
NL	Number of transmission lines
NU	Number of units (unit types include conventional units and renewable energy units)
NU'	Number of equivalent units (unit types include conventional units, renewable energy units, and loads)
NG	Number of conventional units
OC_1, OC_2	Operating costs of original mixed-integer linear programming (MILP) problem (denoted as MILP1) and improved security-constrained unit commitment (SCUC) model (denoted as MILP2)
$\boldsymbol{P}_t^U$	NU dimensional vector at time t

Manuscript received: March 3, 2021; revised: June 11, 2021; accepted: August 30, 2021. Date of CrossCheck: August 30, 2021. Date of online publication: October 7, 2021.

This work was supported by the National Key R&D Program of China (No. 2017YFB0902200).

Q. Yang, J. Wang (corresponding author), H. Yin, and Q. Li are with the School of Electrical Engineering, Xi'an Jiaotong University, Xi'an, China (e-mail: yangqian4071@stu.xjtu.edu.cn; jxwang@mail.xjtu.edu.cn; yinhongrui@stu.xjtu.edu.cn; liqingtao0228@stu.xjtu.edu.cn).

DOI: 10.35833/MPCE.2021.000155

$P_{i,t}^{D}$ Power demand of load i at time t

$\bar{P}_{i}^{D}$, $\underline{P}_{i}^{D}$ The maximum and minimum power demands of load i during the whole period

$\bar{P}_{i}^{G}$, $\underline{P}_{i}^{G}$ The maximum and minimum operating power of conventional unit i

$\bar{P}_{i}^{R}$, $\underline{P}_{i}^{R}$ The maximum and minimum predicted power of renewable energy unit i during the whole period

$\bar{P}_{i,t}^{R}$ Predicted power of renewable energy unit i at time t

$\bar{P}_{i,t}^{U}$, $\underline{P}_{i,t}^{U}$ The maximum and minimum operating power of unit i at time t

$\bar{P}_{i}^{U'}$, $\underline{P}_{i}^{U'}$ The maximum and minimum operating power of equivalent unit i during the whole period

$\bar{P}_{l}^{L}$ Transmission capacity of line l

q Number of conventional unit types

RU_i, RD_i The maximum ramp-up and ramp-down rates of conventional unit i

SU_i, SD_i Startup and shutdown costs of conventional unit i

T_{i}^{on}, T_{i}^{off} The minimum up and down time of conventional unit i

T Operation time of long-term SCUC

v_m Index of units

W_{i}^{P} Predicted energy of power plant i during the whole period

$z_{i,t}$, $z'_{i,t}$ Numbers of i^{th} type units that are online at time t in MILP1 and MILP2

C. Variables

$d_{i,t}$ Binary shutdown variable for conventional unit i at time t

$P_{i,t}^{G}$ Operating power of conventional unit i at time t

$P_{i,t}^{R}$ Operating power of renewable energy unit i at time t

$P_{i,t}^{R,curt}$ Power curtailment of renewable energy unit i at time t

$P_{i,t}^{U}$ Operating power of unit i at time t

$P_{i}^{U'}$ Operating power of equivalent unit i

$u_{i,t}$ Binary startup variable for conventional unit i at time t

$x_{i,t}$ Binary variable, which is equal to 1 if conventional unit i is online at time t and 0 otherwise

I. Introduction

RECENTLY, the penetration rate of renewable energy has increased rapidly. However, renewable energy has strong randomness and volatility, which will bring difficulties to the planning and operation of power systems [1]-[3]. As day-ahead dispatch can only arrange the unit generation plan to deal with the short-term randomness of renewable energy, it cannot fully consider the long-term volatility. Due to the large-scale renewable energy integration, conventional units may frequently start up and shut down to perform peak shaving and valley filling. If the unit generation plan is not coordinated on a long-term scale, the unit status arrangement may be unable to cope with the long-term volatility of renewable energy. Therefore, to ensure the sufficient utilization of renewable energy, reasonable arrangement for the long-term power generation plan has become more crucial. Security-constrained unit commitment (SCUC) is a critical technical means to optimize the long-term scale power generation plan.

SCUC can be described as a mixed-integer linear programming (MILP) problem. For the studies of SCUC, most researchers focus on the short-term scale [4]-[10] such as day-ahead optimization scheduling, but it is difficult to consider the long-term volatility of renewable energy as it optimizes the power generation plan on a daily basis. In long-term SCUC, the volatility of renewable energy and the economy of system operation can be taken into account in the time scale of one week, one month, or even longer, which can make a reasonable power generation plan to ensure the sufficient utilization of renewable energy. However, long-term SCUC is computationally intractable because it has plenty of variables and intertemporal constraints. In order to make long-term SCUC suitable for engineering applications, the computational efficiency must be improved. Therefore, it is necessary to propose a fast calculation method for long-term SCUC.

In the existing research, the methods to reduce the difficulty in the long-term SCUC calculation can be mainly categorized as complex constraint processing, binary variable reduction, and temporal decomposition. Regarding the complex constraints of conventional units, decomposition algorithms with iterative calculation are widely adopted. Reference [11] uses the Lagrangian relaxation algorithm to relax the complex constraints, thereby decomposing the original problem into independent subproblems to solve. Based on Lagrangian relaxation, [12] and [13] use the Dantzig-Wolfe decomposition algorithm to make the convergence more stable.

For binary variable reduction, [14] and [15] develop a relaxation-induced approach to accelerate the search for the optimal unit statuses. This approach adds a penalty term for unit statuses to the objective function, which can effectively improve the calculation efficiency when selecting appropriate parameters. References [16]-[18] establish the clustered unit commitment (CUC) model, which can greatly reduce the binary variables and intertemporal constraints. The CUC model does not have a complicated iterative process, and directly makes a reasonable simplification of unit commitment (UC), which has a strong advantage in stable calculation without consideration of network security constraints.

For temporal decomposition, [19] designs a parallel computing framework to decompose the original problem into multiple subproblems with a short period. In order to obtain a feasible solution, it adopts certain measures to correct the coupling relationship of unit statuses between adjacent subproblems. Reference [20] develops an accelerated analytical target cascading algorithm to solve the subproblems in parallel, which can ensure the feasibility of the solution without additional processing. These methods are effective without

consideration of the energy constraints of conventional units during the whole period.

Many research works have been conducted to reduce the difficulty of the long-term SCUC calculation. Besides, the complexity of network security constraints is also an important factor that can make the problem intractable, especially in the face of large-scale power systems. For the processing of network constraints, [21] simplifies the complex SCUC model as a linear programming (LP) problem, and applies duality theory to directly obtain the analytical sufficient condition for identifying redundant constraints, which will no longer need to solve any optimization model. This method can identify most of the redundant constraints only by the simple mathematical calculation based on the system load and grid parameters, which is very efficient. With the increase of the component types, the redundant constraint identification (RCI) criterion needs to be modified to ensure generality. Moreover, as the time scale of SCUC increases, the elapsed time in the RCI process will also increase. Therefore, the RCI process needs to be improved in long-term SCUC.

In engineering applications, the iterative processes and penalty parameters may affect the stability of the calculation, whereas some stable methods should ignore important constraints, which may lead to the infeasibility of the optimal solution. Therefore, the contradiction between calculation efficiency and solution accuracy is inevitable. In the case of increasing the calculation speed, it is easy to cause deviations in the solution. For long-term SCUC, engineering applications prefer the methods that are easy to set up parameters, are stable in the calculation process, and can get a feasible solution. However, existing methods cannot satisfy all of these characteristics. Therefore, we develop a fast calculation method for long-term SCUC of large-scale power systems with renewable energy, which can satisfy all of these characteristics. The main contributions are as follows.

1) A method of unit status reduction based on temporal decomposition for long-term SCUC is proposed. First, the linear relaxation problem is solved and a boundary condition generation strategy for unit status reduction in SCUC is formulated. Then, the number of binary variables and intertemporal constraints in SCUC can be reduced by the boundary conditions, so as to improve calculation efficiency while obtaining a high-precision feasible solution.

2) An improved RCI method is proposed, which can be used to process the components whose power ranges change over time, thereby reducing the scale of network security constraints and further improving the calculation efficiency of SCUC.

3) A joint accelerated calculation framework for unit status reduction and RCI is formed. A rapid identification technique for RCI is proposed, which is well adapted to long-term calculations. Furthermore, unit status reduction can enhance the effect of RCI, so as to create additional acceleration benefits for the calculation process.

The remainder of this paper is organized as follows. Section II describes the complete long-term SCUC model. In Section III, a method for unit status reduction based on temporal decomposition for long-term SCUC is proposed. Section IV develops the RCI method. In Section V, a joint accelerated calculation framework for long-term SCUC is designed. Section VI analyzes the numerical results of two test systems (ROTS2017 and NREL-118) and verify the effectiveness of the proposed calculation method. Finally, the conclusions are drawn in Section VII.

II. Long-term SCUC Model

The original MILP problem, denoted as MILP1, can be represented as a complete long-term SCUC model [10], [15], which is established on the premise of the known power grid planning scheme, power supply planning scheme, load forecasting, and maintenance schedule. Compared with short-term SCUC, long-term SCUC should consider the energy constraints of power plants over the whole period, which can be expressed as:

$$\left| \sum_{t\in\Omega_T}\sum_{j\in\Omega_{P,i}} P_{j,t}^{G}\Delta t - W_i^P \right| \le \sigma^P W_i^P \quad \forall i\in\Omega_P \tag{1}$$

The objective function and residual constraints are shown in (2)-(13).

$$\min \sum_{t\in\Omega_T}\left[\sum_{i\in\Omega_G}\left(C_i(P_{i,t}^G)\Delta t + SU_i\cdot u_{i,t} + SD_i\cdot d_{i,t}\right) + \beta^R \sum_{i\in\Omega_R} P_{i,t}^{R,curt}\Delta t \right] \tag{2}$$

s.t.

$$x_{i,t} - x_{i,t-1} = u_{i,t} - d_{i,t} \quad \forall i\in\Omega_G, \forall t\in\Omega_T \tag{3}$$

$$x_{i,t}\underline{P}_i^G \le P_{i,t}^G \le x_{i,t}\bar{P}_i^G \quad \forall i\in\Omega_G, \forall t\in\Omega_T \tag{4}$$

$$P_{i,t}^G - P_{i,t-1}^G \le RU_i + u_{i,t}\left(\underline{P}_i^G - RU_i\right) \quad \forall i\in\Omega_G, \forall t\in\Omega_T \tag{5}$$

$$P_{i,t-1}^G - P_{i,t}^G \le RD_i + d_{i,t}\left(\underline{P}_i^G - RD_i\right) \quad \forall i\in\Omega_G, \forall t\in\Omega_T \tag{6}$$

$$\sum_{j=t}^{t-T_i^{on}-1} x_{i,j} \ge u_{i,t}T_i^{on} \quad \forall i\in\Omega_G, \forall t\in\Omega_T \tag{7}$$

$$\sum_{j=t}^{t-T_i^{off}-1} \left(1-x_{i,j}\right) \ge d_{i,t}T_i^{off} \quad \forall i\in\Omega_G, \forall t\in\Omega_T \tag{8}$$

$$0 \le P_{i,t}^R \le \bar{P}_{i,t}^R \quad \forall i\in\Omega_R, \forall t\in\Omega_T \tag{9}$$

$$P_{i,t}^{R,curt} = \bar{P}_{i,t}^R - P_{i,t}^R \quad \forall i\in\Omega_R, \forall t\in\Omega_T \tag{10}$$

$$\sum_{i\in\Omega_G} P_{i,t}^G + \sum_{i\in\Omega_R} P_{i,t}^R = \sum_{i\in\Omega_D} P_{i,t}^D \quad \forall t\in\Omega_T \tag{11}$$

$$\sum_{i\in\Omega_G}\left(\bar{P}_i^G - P_{i,t}^G\right) \ge \alpha^{RS}\sum_{i\in\Omega_D} P_{i,t}^D \quad \forall t\in\Omega_T \tag{12}$$

$$-\bar{P}_l^L \le \sum_{i\in\Omega_G} F_{l,i}^G P_{i,t}^G + \sum_{i\in\Omega_R} F_{l,i}^R P_{i,t}^R - \sum_{i\in\Omega_D} F_{l,i}^D P_{i,t}^D \le \bar{P}_l^L \quad \forall l\in\Omega_L, \forall t\in\Omega_T \tag{13}$$

The objective function (2) includes the operating cost of conventional units and the power curtailment cost of renewable energy units. The operating cost of conventional units consists of generation cost, startup cost, and shutdown cost.

Constraints (3)-(8) are the operation constraints of conven-

tional units. Among them, (3) represents the relationship between binary variables; (4) limits the output range; (5) and (6) represent the ramp rate constraints; and (7) and (8) are the minimum up and down time constraints, respectively.

Constraint (9) limits the output range of renewable energy units, and (10) shows the expression of power curtailment of renewable energy units.

Constraint (11) is the system power balance constraint. Constraint (12) reflects the system reserve capacity demand. Constraint (13) is the network security constraint.

The generation cost function $C_i(\cdot)$ is usually expressed as a quadratic function. In this paper, we will piecewise linearize $C_i(\cdot)$ and treat generation cost as a variable, denoted as $c_{i,t}$. The generation cost constraint can be expressed as:

$$c_{i,t} \geq k_{i,j} P_{i,t}^G + x_{i,t} h_{i,j} \quad \forall i \in \Omega_G,\ j = 1, 2, \ldots, n,\ \forall t \in \Omega_T \tag{14}$$

III. Unit Status Reduction Based on Temporal Decomposition

For MILP1, the number of binary variables and intertemporal constraints (7) and (8) for conventional units will heavily affect the model solution. Therefore, we develop a method to reduce binary variables and intertemporal constraints in this section.

A. Linearized Relaxation

In order to quickly obtain an approximate solution, we apply the linear relaxation to MILP1. This new problem is a purely LP problem, denoted as LP1.

In LP1, all binary variables of MILP1 will be serialized [14]. Compared with MILP1, the following additional constraints of LP1 are required:

$$\begin{cases} 0 \leq x_{i,t} \leq 1 \\ 0 \leq u_{i,t} \leq 1 \\ 0 \leq d_{i,t} \leq 1 \end{cases} \quad \forall i \in \Omega_G,\ \forall t \in \Omega_T \tag{15}$$

Obviously, the solution space of LP1 is the convex hull of the solution space of MILP1, which makes the optimal solution of LP1 provide a lower bound for the optimal solution of MILP1.

B. Boundary Condition Design

Due to the linear characteristics of LP1, the optimal solution of LP1 may be infeasible for MILP1. Nevertheless, LP1 can still provide an approximate solution close to the optimal solution of MILP1, which can become good boundary conditions to solve MILP1 efficiently after some treatment. The specific processes are as follows.

1) Set Thresholds

According to the description in [15], although the conventional unit statuses are continuous in LP1, $x_{i,t}$ in MILP1 will tend to be 1 when $x_{i,t}$ in LP1 is a large fractional number and vice versa. This idea is applied to design the boundary conditions in this paper. If the unit output is greater than a threshold, the unit status is determined to be on, and if the unit output is less than another threshold, the unit status is determined to be off.

The output thresholds of conventional units are set as α and β, which range from [0, 1]. The output of unit i at time t obtained by LP1 is $\tilde{P}_{i,t}^G$. We assume that when $\tilde{P}_{i,t}^G \leq \alpha \underline{P}_i^G$, unit i should remain in off state at time t, and when $\tilde{P}_{i,t}^G \geq \underline{P}_i^G + \beta\left(\bar{P}_i^G - \underline{P}_i^G\right)$, unit i should remain in on state at time t. The constraints can be described as:

$$\begin{cases} x_{i,t} = 0 & \tilde{P}_{i,t}^G \leq \alpha \underline{P}_i^G,\ \forall t \in \Omega_T \\ x_{i,t} = 1 & \tilde{P}_{i,t}^G \geq \underline{P}_i^G + \beta\left(\bar{P}_i^G - \underline{P}_i^G\right),\ \forall t \in \Omega_T \end{cases} \tag{16}$$

2) Status Reduction Rule

Since the statuses of conventional units determined one by one according to a single time t may not meet the minimum up and down time constraints, the generated boundary conditions will cause no solution to MILP1. To solve this problem, we refer to the idea of temporal decomposition in [19] to determine the unit statuses. According to the operating parameters of each conventional unit, we decompose the whole period into multiple short periods with the same time scale.

For the convenience of description, we define a short period as period s, and the time scale in it is denoted as T_s. Therefore, the following relationship holds:

$$s = \left\{ t \in \Omega_T \middle| t = T_s(s-1) + 1, T_s(s-1) + 2, \ldots, T_s s \right\} \tag{17}$$

For m periods after period s, they can be respectively expressed as $\{s+1,\ s+2, \ldots, s+m-1, s+m\}$. The rule of unit status reduction is as follows.

For unit i, the average operating power in period s obtained by LP1 is $\tilde{P}_{i,s}^G$. If it satisfies $\tilde{P}_{i,s}^G \leq \alpha \underline{P}_i^G$, unit i should remain in off state in period s. In the same way, if it satisfies $\tilde{P}_{i,s}^G \geq \underline{P}_i^G + \beta\left(\bar{P}_i^G - \underline{P}_i^G\right)$, unit i should remain in on state in period s. The constraints on the determined statuses for unit i in period s are as follows:

$$\begin{cases} x_{i,t} = 0 & \tilde{P}_{i,s}^G \leq \alpha \underline{P}_i^G,\ \forall t \in s \\ x_{i,t} = 1 & \tilde{P}_{i,s}^G \geq \underline{P}_i^G + \beta\left(\bar{P}_i^G - \underline{P}_i^G\right),\ \forall t \in s \end{cases} \tag{18}$$

For different units, the number of hours included in each short period can be different. However, it should be noted that at least $\max\{T_i^{on}, T_i^{off}\}$ hours are included in period s, so as to ensure that unit i can meet the minimum up and down time constraints if the statuses are determined in period s.

Next, the periods of undetermined statuses are further analyzed. For unit i, we suppose that the two adjacent periods of determined statuses are s and $s+m$, respectively, then the intermediate periods of undetermined statuses are $\{s+1,\ s+2,\ \ldots,\ s+m-1\}$ as shown in Fig. 1. Among them, we assume that the initial time of period $s+1$ is t_1, and the initial time of period $s+m$ is t_2.

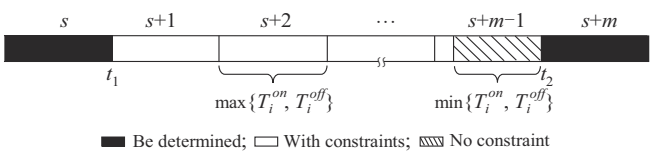

Fig. 1. The minimum up and down time constraints in different periods.

For time t_1, since the statuses in period s already satisfy the minimum up and down time constraints, the status at t_1 can be changed without any constraints by period s, which

indicates that the normal minimum up and down time constraints can be added starting from t_1. Therefore, we only need to consider the coupling relationship between the statuses in period $s+m-1$ and the initial status x_{i,t_2} in period $s+m$.

For the period $[t_2-T_i^{on}+1,\ t_2-1]$, because this period is less than T_i^{on} hours, if $x_{i,t}$ changes from 0 to 1 during this period, the minimum up time constraints must not be satisfied when $x_{i,t_2}=0$. Therefore, the following constraints must be satisfied.

$$u_{i,t}=0 \quad x_{i,t_2}=0,\ t=t_2-T_i^{on}+1,\ldots,t_2-1 \tag{19}$$

In the same way, for the period $[t_2-T_i^{off}+1,\ t_2-1]$, because this period is less than T_i^{off} hours, if $x_{i,t}$ changes from 1 to 0 during this period, the minimum down time constraints must not be satisfied when $x_{i,t_2}=1$. Therefore, the following constraints must be satisfied:

$$d_{i,t}=0 \quad x_{i,t_2}=1,\ t=t_2-T_i^{off}+1,\ldots,t_2-1 \tag{20}$$

For the period $[t_2-\tilde{T}_i+1,\ t_2-1]$, when $x_{i,t_2}=0$, the constraint $u_{i,t}=0$ based on (19) makes (7) unconstrained and $x_{i,t}$ cannot change from 0 to 1, thus there are 3 situations for $x_{i,t}$ as shown in Fig. 2: ① keep 0 unchanged (situation 1); ② keep 1 unchanged (situation 2); and ③ change from 1 to 0 (situation 3). For situations 1 and 2, $d_{i,t}$ will keep 0 unchanged in the period $[t_2-\tilde{T}_i+1,\ t_2-1]$, thus (8) is unconstrained; and for situation 3, if $x_{i,t}$ changes from 1 to 0 at $t_3\in[t_2-\tilde{T}_i+1,\ t_2-1]$, due to the limit of (19), $x_{i,t}$ will keep 0 unchanged from t_3 to the end time of period $s+m$, thus making (8) always hold, where $\tilde{T}_i=\min\{T_i^{on},\ T_i^{off}\}$. In the same way, when $x_{i,t_2}=1$, the constraint $d_{i,t}=0$ makes (8) unconstrained, and $x_{i,t}$ may remain unchanged or change from 0 to 1, which can make (7) always hold.

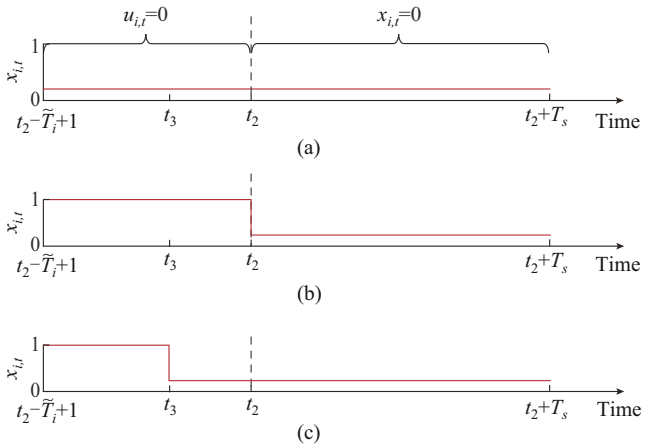

Fig. 2. Unit status values in different situations. (a) Situation 1. (b) Situation 2. (c) Situation 3.

Through the above analyses, for periods $\{s+1,\ s+2,\ \ldots,\ s+m-1\}$, the minimum up and down time constraints do not need to be added at each time, as shown in Fig. 1. The specific constraints can be expressed as:

$$\begin{cases} \sum_{j=t}^{t-T_i^{on}-1} x_{i,j} \ge u_{i,t}T_i^{on} \\ \sum_{j=t}^{t-T_i^{off}-1} \left(1-x_{i,j}\right) \ge d_{i,t}T_i^{off} \end{cases} \quad t=t_1,t_1+1,\ldots,t_2-\tilde{T}_i \tag{21}$$

3) Improved SCUC Model

After solving LP1 and designing boundary conditions, an improved SCUC model called MILP2 is obtained, which can be solved quickly. For unit i, each short period has $\max\{T_i^{on},\ T_i^{off}\}$ hours. Compared with MILP1, the minimum up and down time constraints for MILP2 need to replace (7) and (8) with (18)-(21) for any conventional unit.

It can be observed that MILP2 can flexibly adjust α and β to balance calculation accuracy and efficiency while ensuring a strictly feasible solution of MILP1. When α rises or β falls, the number of determined statuses will increase, and the number of binary variables and intertemporal constraints of MILP2 will decrease, thereby increasing the calculation efficiency. However, the more the number of determined statuses, the greater the probability of unreasonable boundary conditions, which leads to a decrease in the accuracy of the solution. In the same way, when α falls or β rises, the accuracy will increase and efficiency will decrease. If take $\alpha<0$ and $\beta>1$, MILP2 is equivalent to MILP1. Therefore, α and β should range from 0 to 1 to improve the calculation efficiency of MILP2.

IV. RCI Method

For large-scale power systems, network constraints will also bring a great computational burden to the long-term SCUC model. Therefore, we develop the RCI method presented in [21] and make it suitable for components whose power ranges change over time in this section.

First of all, we express the power of all units uniformly, and the transformation form of constraint (13) is as follows:

$$\begin{cases} \sum_{i=1}^{NU} F_{l,i}^U P_{i,t}^U \le \bar{P}_l^L + \sum_{i\in\Omega_D} F_{l,i}^D P_{i,t}^D \\ -\sum_{i=1}^{NU} F_{l,i}^U P_{i,t}^U \le \bar{P}_l^L - \sum_{i\in\Omega_D} F_{l,i}^D P_{i,t}^D \end{cases} \quad \forall l\in\Omega_L,\ \forall t\in\Omega_T \tag{22}$$

The compact form of (22) is as follows:

$$\boldsymbol{F}^U\boldsymbol{P}_t^U \le \boldsymbol{\Gamma}_t \quad \forall t\in\Omega_T \tag{23}$$

The specific forms of $\boldsymbol{F}^U$, $\boldsymbol{P}_t^U$, and $\boldsymbol{\Gamma}_t$ can be expressed as:

$$\boldsymbol{F}^U=\begin{bmatrix} F_{1,1}^U & F_{1,2}^U & \cdots & F_{1,NU}^U \\ F_{2,1}^U & F_{2,2}^U & \cdots & F_{2,NU}^U \\ \vdots & \vdots & & \vdots \\ F_{NL,1}^U & F_{NL,2}^U & \cdots & F_{NL,NU}^U \\ -F_{1,1}^U & -F_{1,2}^U & \cdots & -F_{1,NU}^U \\ -F_{2,1}^U & -F_{2,2}^U & \cdots & -F_{2,NU}^U \\ \vdots & \vdots & & \vdots \\ -F_{NL,1}^U & -F_{NL,2}^U & \cdots & -F_{NL,NU}^U \end{bmatrix} \tag{24}$$

$$\boldsymbol{P}_t^U=[P_{1,t}^U \quad P_{2,t}^U \quad \cdots \quad P_{NU,t}^U]^{\mathrm{T}} \quad \forall t\in\Omega_T \tag{25}$$

$$\boldsymbol{\Gamma}_t=\begin{bmatrix}\bar{P}_1^L+\sum\limits_{i\in\Omega_D}F_{1,i}^D P_{i,t}^D\\ \bar{P}_2^L+\sum\limits_{i\in\Omega_D}F_{2,i}^D P_{i,t}^D\\ \vdots\\ \bar{P}_{NL}^L+\sum\limits_{i\in\Omega_D}F_{NL,i}^D P_{i,t}^D\\ \bar{P}_1^L-\sum\limits_{i\in\Omega_D}F_{1,i}^D P_{i,t}^D\\ \bar{P}_2^L-\sum\limits_{i\in\Omega_D}F_{2,i}^D P_{i,t}^D\\ \vdots\\ \bar{P}_{NL}^L-\sum\limits_{i\in\Omega_D}F_{NL,i}^D P_{i,t}^D\end{bmatrix}\quad\forall t\in\Omega_T \tag{26}$$

In a power system only containing conventional units, when the operating statuses of unit i are not determined in advance, the output range at each time can be represented by $[0, \bar{P}_i^G]$ [21].

Since the maximum output of renewable energy units will change over time, the maximum output of unit i at time t should be modified when renewable energy units exist in the power system. For the minimum output of renewable energy unit i, it should be 0 because the power curtailment is allowed. Therefore, the output range of renewable energy unit i at time t can be represented by $[0, \bar{P}_{i,t}^R]$.

Moreover, for MILP2, the output range of conventional units whose statuses are determined by LP1 will also change dynamically. Therefore, to make the criterion more general, the minimum and maximum outputs of unit i at time t are expressed as $\underline{P}_{i,t}^U$ and $\bar{P}_{i,t}^U$, which can even take negative values. For conventional unit i in MILP2, the following relationships are established:

$$\begin{cases}\underline{P}_{i,t}^U=0\\ \bar{P}_{i,t}^U=0\end{cases}\quad x_{i,t}=0 \tag{27}$$

$$\begin{cases}\underline{P}_{i,t}^U=\underline{P}_i^G\\ \bar{P}_{i,t}^U=\bar{P}_i^G\end{cases}\quad x_{i,t}=1 \tag{28}$$

$$\begin{cases}\underline{P}_{i,t}^U=0\\ \bar{P}_{i,t}^U=\bar{P}_i^G\end{cases}\quad x_{i,t}\text{ is undetermined} \tag{29}$$

For the j^{th} row vector $\boldsymbol{F}_j^U=[f_{j,1}^U, f_{j,2}^U, \ldots, f_{j,NU}^U]^{\mathrm{T}}$ of $\boldsymbol{F}^U$, we sort the elements with the new subscript index as:

$$f_{j,v_1}^U\geq f_{j,v_2}^U\geq\ldots\geq f_{j,v_m}^U\geq\ldots\geq f_{j,v_{NU}}^U\quad j=1,2,\ldots,2NL \tag{30}$$

We can figure out that if there is an integer $k\in[1,NU]$ which satisfies the conditions (31) and (32), the constraint $\boldsymbol{F}_j^U\boldsymbol{P}_t^U\leq\gamma_{j,t}$ is redundant. The above criterion can be easily obtained by the proof process in [21].

$$\underline{P}_{v_k,t}^U\leq D_t-\left(\sum_{m=1}^{k-1}\bar{P}_{v_m,t}^U+\sum_{m=k+1}^{NU}\underline{P}_{v_m,t}^U\right)\leq\bar{P}_{v_k,t}^U \tag{31}$$

$$f_{j,v_k}^U D_t+\sum_{m=1}^{k-1}\left(f_{j,v_m}^U-f_{j,v_k}^U\right)\bar{P}_{v_m,t}^U+\sum_{m=k+1}^{NU}\left(f_{j,v_m}^U-f_{j,v_k}^U\right)\underline{P}_{v_m,t}^U\leq\gamma_{j,t} \tag{32}$$

V. Joint Accelerated Calculation Framework

To maximize the computational efficiency of long-term SCUC, it is necessary to design a joint accelerated computation framework by combining the unit status reduction method with the RCI method. However, the RCI criterion in Section IV needs to be judged on the security constraints for each line at each time. Therefore, with the increase of the number of lines and time periods, the elapsed time of the RCI process will also increase. Based on the above analyses, the RCI process needs to be improved to make it suitable for long-term SCUC.

A. Rapid Identification Technique

The elapsed time of the RCI process is related to the number of node components and the time scale of long-term SCUC. However, it is difficult to reduce the number of node components because the power ranges of all node components are related to the RCI criterion.

For the time scale of long-term SCUC, if we can identify the redundant network constraints during the whole period by just one identification, the time will be saved very significantly. For line l, its power range can reach the maximum value when the power range of each node component is set to be the maximum value. Under this premise, if the network constraint of line l is redundant during the whole period, then the constraint is redundant at each time in long-term SCUC.

According to the above analyses, the preidentification of the whole period is carried out, and the power range of each node component is extended to the maximum value during the whole period. For conventional unit i, the power range is $[0, \bar{P}_i^G]$. For renewable energy units and loads, the power ranges can be expressed as:

$$\begin{cases}\underline{P}_i^R=0 & \forall i\in\Omega_R\\ \bar{P}_i^R=\max\bar{P}_{i,t}^R & \forall i\in\Omega_R,\forall t\in\Omega_T\\ \underline{P}_i^D=\min P_{i,t}^D & \forall i\in\Omega_D,\forall t\in\Omega_T\\ \bar{P}_i^D=\max P_{i,t}^D & \forall i\in\Omega_D,\forall t\in\Omega_T\end{cases} \tag{33}$$

Then, we treat all loads as equivalent units with negative power, and the power balance constraint can be expressed as:

$$\sum_{i=1}^{NU'}P_i^{U'}=0 \tag{34}$$

Therefore, if there exists an integer $k\in[1,NU']$ which satisfies the constraints (35) and (36), the constraint $\boldsymbol{F}_j^U\boldsymbol{P}_t^U\leq\gamma_{j,t}$ is redundant at any time t.

$$\underline{P}_{v_k}^{U'}\leq-\left(\sum_{m=1}^{k-1}\bar{P}_{v_m}^{U'}+\sum_{m=k+1}^{NU'}\underline{P}_{v_m}^{U'}\right)\leq\bar{P}_{v_k} \tag{35}$$

$$\sum_{m=1}^{k-1}\left(f_{j,v_m}^{U'}-f_{j,v_k}^{U'}\right)\bar{P}_{v_m}^{U'}+\sum_{m=k+1}^{NU'}\left(f_{j,v_m}^{U'}-f_{j,v_k}^{U'}\right)\underline{P}_{v_m}^{U'}\leq\bar{P}_j^L \tag{36}$$

Finally, for the constraints that are not judged to be redundant in the preidentification process, the RCI calculation at each time t will be carried out. Since there are only a few constraints that need to be identified at each time t, the computational burden is very small.

B. Calculation Framework

It is worth mentioning that the boundary conditions of MILP2 limit the output range of some conventional units, which causes the power range of each line to be reduced. Therefore, the RCI process of MILP2 can continue to identify the remaining constraints which are not redundant in the identification results of LP1.

Obviously, when the number of determined statuses increases in the boundary conditions, the more redundant network constraints will be identified, which can create additional acceleration benefits for the calculation process of long-term SCUC. Based on the above analyses, we embed the RCI process into the calculation of LP1 and MILP2, respectively, thereby forming the joint accelerated calculation framework for long-term SCUC, as shown in Fig. 3.

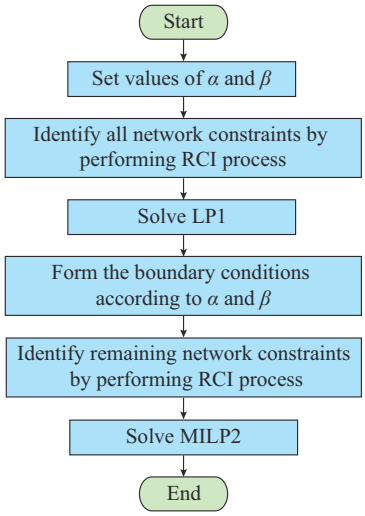

Fig. 3. Joint accelerated calculation framework for long-term SCUC.

VI. Case Studies

In this section, the effectiveness of the proposed calculation method in this paper is first verified by a series of numerical analyses of ROTS2017. Then, we further test the method on the NREL-118 system to prove its scalability. All calculations are performed by CPLEX 12.80 in the C++ environment on a computer equipped with an Intel Core i7-10700 2.90 GHz processor. For all the following cases, the calculation time scale of long-term SCUC is set to be 672 hours (4 weeks), and the convergence gap is set to be 10^{-5}.

For the long-term SCUC model, the initial values we need to set contain the operating status and power of conventional units at the initial moment as well as the duration that conventional units have been kept on or off. The above initial value does not affect the convergence speed but will affect the optimal solution of the model. In order to make the model independent of the initial value as much as possible, we assume that: ① the initial operating status of all units is on; ② the duration of keeping on exceeds the minimum up time; and ③ the ramp rate constraints at the first moment of the model are relaxed. Therefore, all units can change the status and adjust to any operating power at the first moment.

A. ROTS2017

In this case, ROTS2017 is tested to verify the validity of the proposed method. This system consists of 44 buses, 63 lines, 42 conventional units (including coal-fired units and hydro units), and 9 renewable energy units. The detailed data of this system can be freely accessed in [22].

To highlight the characteristics of high penetration of renewable energy, we double the installed capacity of renewable energy and the transmission capacity directly connected to the renewable energy units, and increase the load level by 1.2 times, so that the proportion of renewable energy installed can be increased to 37%. For hydro units without operating cost, binary variables and related constraints are not set due to their high operational flexibility.

First, we will show the effect of RCI in MILP1 and LP1. Next, based on the application of the joint accelerated computation framework, we will analyze the calculation performance of MILP2 under different values of α and β, including the calculation efficiency and the accuracy of the optimal solution. Finally, we will select the case with the best overall effect and make further comparative analyses of the operation results.

1) Effect of RCI

The effect of RCI in MILP1 and LP1 is shown in Table I. The proportion of redundant network constraints to all network constraints is named redundancy ratio. It can be observed that more than 98% of the network constraints are redundant, and by reducing these constraints, both MILP1 and LP1 have been significantly improved in calculation efficiency. Furthermore, for both MILP1 and LP1 problems, the operating cost of the case with RCI is the same as that without RCI, which can verify that RCI does not affect the optimal objective value.

TABLE I
Effect of RCI in MILP1 and LP1

Model	RCI process	Operating cost (RMB)	Elapsed time (s)	Redundancy ratio (%)
MILP1	With	766234000	2654.68	98.39
MILP1	Without	766234000	3728.04	
LP1	With	764985000	18.76	98.39
LP1	Without	764985000	54.42	

For LP1 and MILP1, the RCI process includes the preidentification of all lines during the whole period and the identification of the remaining lines at each time. Among them, the preidentification can identify that 80.67% of the network constraints are redundant, which takes 1.09 s to complete the calculation. Then, 17.72% of the network constraints are further identified as redundancy by the identification of the remaining lines at each time, which takes 0.82 s to complete the calculation. If all lines are directly identified at each time, the calculation time will exceed 5 s. The effect is not obvious for this system, but for a system with a larger network frame, the RCI process in this paper will be more efficient. We will show this effect in Section VI-B.

In addition, the optimal operating costs of LP1 and MILP1 are 7.64985×10^8 RMB and 7.66234×10^8 RMB, respectively. The relative error of operating cost between LP1 and MILP1 is only –0.163%. It can be observed that the optimal solution of LP1 can provide a lower bound for the optimal solution of MILP1, and they are very close to each other. The subsequent analyses will be based on the joint accelerated calculation framework.

2) Results Under Different Values of α and β

Based on the solution of LP1, different values are set for the output thresholds α and β to solve MILP2, and the accuracy and efficiency are compared with MILP1. As the benchmark, MILP1 is named Case 0, which does not require unit status reduction. For MILP2 with different values of α and β, they correspond to Case 1 to Case 9, respectively. The specific comparison results are shown in Table II and Fig. 4.

TABLE II
COMPARISON BETWEEN DIFFERENT CASES

Case	Output threshold	Operating cost (RMB)	REOC (%)	SRR (%)	DSR (%)	Redundancy ratio (%)	Elapsed time (s)	Acceleration ratio	CRRE (%)
Case 0	Benchmark	766234000				98.39	2654.68	1.00	0.623
Case 1	$\alpha=0.9,\beta=0.1$	826696000	7.891	84.06	9.14	99.88	7.25	366.27	0.223
Case 2	$\alpha=0.8,\beta=0.2$	783980000	2.316	73.97	6.95	99.80	19.43	136.63	0.149
Case 3	$\alpha=0.7,\beta=0.3$	772243000	0.784	66.92	4.20	99.80	46.76	56.77	0.354
Case 4	$\alpha=0.6,\beta=0.4$	769785000	0.463	57.17	2.53	99.73	65.83	40.33	0.654
Case 5	$\alpha=0.5,\beta=0.5$	766412000	0.023	45.71	1.92	99.63	167.60	15.84	0.638
Case 6	$\alpha=0.4,\beta=0.6$	766359000	0.016	39.45	1.79	99.51	202.98	13.08	0.645
Case 7	$\alpha=0.3,\beta=0.7$	766313000	0.010	23.46	1.62	98.96	416.42	6.38	0.605
Case 8	$\alpha=0.2,\beta=0.8$	766281000	0.006	12.49	1.17	98.61	921.05	2.88	0.640
Case 9	$\alpha=0.1,\beta=0.9$	766257000	0.003	5.43	0.85	98.46	2207.27	1.20	0.634
Case 10	$\alpha=0.5,\beta=0.5$	766412000	0.023	45.71	1.92		355.23	7.47	0.638

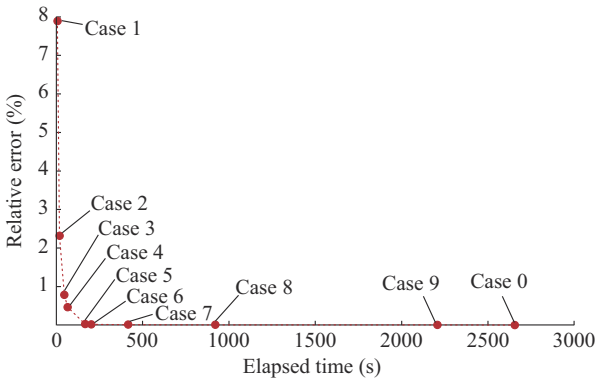

Fig. 4. Calculation results of each case.

Among them, the relative error in operating cost (REOC) between MILP1 and MILP2 can be expressed as:

$$REOC=\left(OC_2-OC_1\right)/OC_1\times100\% \tag{37}$$

The status reduction ratio (SRR) represents the proportion of the determined unit statuses in boundary conditions to the total unit statuses. The difference status ratio (DSR) is defined as the ratio of the number of different statuses between MILP1 and MILP2 to the total number of unit statuses, which can be calculated as:

$$DSR=\sum_{i=1}^{q}\sum_{t=1}^{T}\left|z'_{i,t}-z_{i,t}\right|\Big/\left(T\cdot NG\right)\times100\% \tag{38}$$

In this test system, we regard the units with the same installed capacity as the same type. The acceleration ratio is defined as the ratio of MILP1 to MILP2 in the elapsed time. The curtailment ratio of renewable energy (CRRE) can be calculated as:

$$CRRE=\sum_{i\in\Omega_R}\sum_{t\in\Omega_T}P_{i,t}^{R,curt}\Big/\sum_{i\in\Omega_R}\sum_{t\in\Omega_T}\bar{P}_{i,t}^{R}\times100\% \tag{39}$$

As can be observed from Table I, the MILP1 without RCI needs 3728.04 s to solve the long-term SCUC. For the joint accelerated calculation framework proposed in this paper, LP1 with RCI only needs 18.76 s to solve the linear relaxation problem, and the average elapsed time of all MILP2 cases with RCI is less than 1000 s, as shown in Table II. Even for Case 9, which takes the most time of MILP2 with RCI, the total elapsed time (2226.03 s) with the LP1 process is much less than that of the MILP1. Therefore, the calculation of joint accelerated calculation framework is faster than the MILP1.

For MILP2, it will continue to carry out the RCI calculation based on the RCI results of LP1. At this time, we only need to identify the remaining 1.61% of network constraints one by one, which requires a small amount of calculation. As the values of α and β are adjusted to increase SRR, the redundancy ratio will also increase, which results in the further reduction of binary variables and network constraints in MILP2, as shown in Table II. This proves that the joint accelerated calculation framework has additional acceleration benefits for the calculation process of long-term SCUC.

To further verify the effectiveness of RCI, Case 10 ($\alpha=0.5$, $\beta=0.5$) without RCI is designed. It can be observed from Table II that the optimization results of Case 5 are the same as those of Case 10, but Case 5 consumes less time than Case 10, which verifies that RCI can improve the computational efficiency and does not affect the optimization results.

For the accuracy of the results, it can be observed from Table II and Fig. 4, as the efficiency of MILP2 increases,

the accuracy will decrease due to the deviation caused by the determined unit statuses. When SRR is 30%-50%, it will considerably affect this test system (like Case 5), which can improve the calculation speed by more than 15 times with REOC of only 0.023%. When SRR is less than 20%, it will increase much calculation time for less than 1/10000 precision, which is not necessary for engineering applications that do not require high precision. Due to the different boundary conditions of conventional units in each case, CRRE will be different. However, with the decrease of REOC, CRRE will also be stable and close to the benchmark result.

For the values of DSR between different cases, most of the on/off statuses of the units are the same as shown in Table II. In addition, DSR will rise with the increase of SRR, which shows that the more unit statuses are determined by the boundary conditions, the more deviations to the optimal unit statuses will occur.

In order to visually compare the unit statuses between different cases, we show the number of online units of different types between Case 0 and Case 5 in ROTS2017 in Fig. 5. Only 1.92% of statuses are different. Among them, the statuses of 300 MW units are all the same, which are online during the whole period due to the large load demand on the buses around them. The 200 MW units are installed in the load area and the 600 MW units are installed in renewable energy intensive areas, respectively. When the load demand or renewable energy output changes dramatically, units need to change their statuses for peak regulation, and there will be no more than 2 units with inconsistent on/off statuses of each type. In Case 5, when the boundary conditions are formulated, some determined units may be different from Case 0 due to the heuristic feature of the proposed calculation method. In addition, when the statuses of a unit are determined within a short period, the moment of status change will occur at the beginning or end of the short period, which may be earlier or later than Case 0. The difference of on/off statuses does not greatly affect the economy of the solution and the value of DSR is very small, which is acceptable for engineering applications.

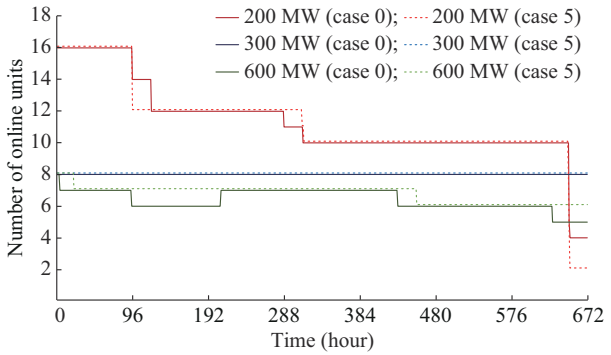

Fig. 5. Number of online units of different types between Case 0 and Case 5 in ROTS2017.

In engineering applications, since the optimal operating cost of MILP1 is unknown, REOC between MILP2 and LP1 can be used to estimate the accuracy of MILP2. Taking Case 5 as an example, REOC is 0.187%. Since the optimal operating cost of MILP1 must be no less than LP1, REOC between MILP2 and MILP1 can be guaranteed to be smaller.

3) Comparative Analyses Between MILP1 and MILP2

According to the above analyses, we select Case 5 as MILP2 for comparative analyses with MILP1. As shown in Table III, the results of average utilization time are provided, which can show the accuracy of operation results at the power supply side. For different types of units, the maximum relative error between MILP1 and MILP2 is only 0.601%. Numerical results show that the relative error of average online hours of 600 MW units is 4.643%, which is larger than the relative error of average utilization time. Compared with the unit statuses, the unit power is continuous at each time and the error of average utilization time can be reduced to a small amount during the optimization process.

TABLE III
RESULTS OF AVERAGE UTILIZATION TIME

Installed capacity (MW)	Average utilization time (hour)		Relative error (%)
	MILP1	MILP2	
200	391.14	393.49	0.601
300	372.06	370.06	–0.537
600	362.52	360.57	–0.537

Furthermore, in order to show the accuracy of operation results at the power grid side, we select the top 10 lines with the highest average load rate, as shown in Table IV. It can be observed that MILP2 can accurately describe the average load rate in terms of value and order. Among them, the absolute value of relative error is less than 0.5% for most lines, which meets the needs of engineering applications.

TABLE IV
RESULTS OF AVERAGE LOAD RATE

Line name	Average load rate (%)		Relative error (%)
	MILP1	MILP2	
C21M-C25	60.27	60.31	0.064
C22H-C22M	51.99	52.02	0.053
C21H-C21M	46.68	46.78	0.207
B17-C21H	46.48	46.55	0.152
C27-C32	45.03	45.65	1.378
A11-B13	41.52	41.39	–0.311
C22M-C28	41.31	41.26	–0.132
C25-C27	41.15	41.19	0.111
C35-C36	32.24	32.18	–0.197
C22M-C30	31.84	31.94	0.291

B. NREL-118

To verify the scalability of the proposed method to different power systems, we select NREL-118 [23] for further testing. The system consists of 118 buses, 186 transmission lines, 54 conventional units, and 92 renewable energy units. The proportion of renewable energy installed is 38.52% in this system.

As the system contains plenty of units and lines, the role of the preidentification will be played significantly. The RCI process can reduce the network constraints of MILP1 by 99.3%. If the preidentification is adopted during the whole period, the modeling time is only 5 s, otherwise, it will exceeds 60 s. If the system scale becomes larger, the modeling time saved with the preidentification will be more significant.

During the test process, we find that when $(\alpha, \beta)=(0.6, 0.4)$ and the statuses of 61.33% are determined, the performance of MILP2 is good. REOC between MILP2 and MILP1 is only 0.015%, while the acceleration ratio reaches 11.89. This is because the fuel types of conventional units including coal, oil, and gas vary significantly in price. Numerical results show that for different types of units, the maximum relative error of average online hours is 0.532%, which is much smaller than the same index in ROTS2017. Therefore, when the difference of economy between different types of units is more obvious, the accuracy of determined statuses will increase, which results in a better quality of the optimal solution in MILP2.

VII. Conclusion

In this paper, a fast calculation method for long-term SCUC of large-scale power systems with renewable energy is proposed. First, by solving the linear relaxation problem and designing the boundary conditions based on temporal decomposition, the status reduction method can reduce binary variables and intertemporal constraints of SCUC. Then, an efficient RCI method is developed to reduce the number of network constraints. Finally, a joint accelerated calculation framework for unit status reduction and RCI is formed.

The results of case studies on ROTS2017 and NREL-118 indicate that when reasonable values of α and β are set, a feasible solution with relative error in the order of 10^{-4} can be obtained, and the calculation speed is more than 10 times faster than the original problem, which meets the requirements of engineering applications. In addition, this method does not have an iterative process and the acceleration effect is stable, which is suitable for engineering applications.

For the RCI method with the preidentification process, it can realize the fast identification of redundant network constraints on a long-term scale. Furthermore, unit status reduction can enhance the effect of the RCI method, thus creating additional acceleration benefits for the calculation of long-term SCUC. It can be concluded that the proposed method has high scalability to accelerate the calculation of long-term SCUC for different power systems, and obtain a high-precision feasible solution.

References

[1] A. Bagheri, C. Zhao, F. Qiu *et al.*, "Resilient transmission hardening planning in a high renewable penetration era," *IEEE Transactions on Power Systems*, vol. 34, no. 2, pp. 873-882, Mar. 2019.

[2] H. Park, R. Baldick, and D. P. Morton, "A stochastic transmission planning model with dependent load and wind forecasts," *IEEE Transactions on Power Systems*, vol. 30, no. 6, pp. 3003-3011, Nov. 2015.

[3] X. Yuan, "Overview of problems in large-scale wind integrations," *Journal of Modern Power Systems and Clean Energy*, vol. 1, no. 1, pp. 22-25, Jul. 2013.

[4] Y. Chen, A. Casto, F. Wang *et al.*, "Improving large scale day-ahead security constrained unit commitment performance," *IEEE Transactions on Power Systems*, vol. 31, no. 6, pp. 4732-4743, Nov. 2016.

[5] M. Zhou, J. Zhai, G. Li *et al.*, "Distributed dispatch approach for bulk AC/DC hybrid systems with high wind power penetration," *IEEE Transactions on Power Systems*, vol. 33, no. 3, pp. 3325-3336, May 2018.

[6] X. Zheng, H. Chen, Y. Xu *et al.*, "A hierarchical method for robust SCUC of multi-area power systems with novel uncertainty sets," *IEEE Transactions on Power Systems*, vol. 35, no. 2, pp. 1364-1375, Mar. 2020.

[7] X. Zhu, Z. Yu, and X. Liu, "Security constrained unit commitment with extreme wind scenarios," *Journal of Modern Power Systems and Clean Energy*, vol. 8, no. 3, pp. 464-472, May 2020.

[8] B. Hu and L. Wu, "Robust SCUC considering continuous/discrete uncertainties and quick-start units: a two-stage robust optimization with mixed-integer recourse," *IEEE Transactions on Power Systems*, vol. 31, no. 2, pp. 1407-1419, Mar. 2016.

[9] H. Ye, J. Wang, and Z. Li, "MIP reformulation for max-min problems in two-stage robust SCUC," *IEEE Transactions on Power Systems*, vol. 32, no. 2, pp. 1237-1247, Mar. 2017.

[10] L. Nan, Y. Liu, L. Wu *et al.*, "Graph theory based *N*–1 transmission contingency selection and its application in security-constrained unit commitment," *Journal of Modern Power Systems and Clean Energy*, vol. 9, no. 6, pp. 1458-1467, Nov. 2021.

[11] K. Aoki, M. Itoh, T. Satoh *et al.*, "Optimal long-term unit commitment in large scale systems including fuel constrained thermal and pumped-storage hydro," *IEEE Transactions on Power Systems*, vol. 4, no. 3, pp. 1065-1073, Aug. 1989.

[12] Y. Fu, M. Shahidehpour, and Z. Li, "Long-term security-constrained unit commitment: hybrid Dantzig-Wolfe decomposition and subgradient approach," *IEEE Transactions on Power Systems*, vol. 20, no. 4, pp. 2093-2106, Nov. 2005.

[13] K. Kim, A. Botterud, and F. Qiu, "Temporal decomposition for improved unit commitment in power system production cost modeling," *IEEE Transactions on Power Systems*, vol. 33, no. 5, pp. 5276-5287, Sept. 2018.

[14] Y. Wang, H. Zhong, Q. Xia *et al.*, "Coordination of generation maintenance scheduling and long-term SCUC with energy constraints and $N-1$ contingencies," *IET Generation, Transmission & Distribution*, vol. 10, no. 2, pp. 325-333, Apr. 2016.

[15] Y. Bai, H. Zhong, Q. Xia *et al.*, "Inducing-objective-function-based method for long-term SCUC with energy constraints," *International Journal of Electrical Power & Energy Systems*, vol. 63, pp. 971-978, Jul. 2014.

[16] G. Morales-España and D. A. Tejada-Arango, "Modeling the hidden flexibility of clustered unit commitment," *IEEE Transactions on Power Systems*, vol. 34, no. 4, pp. 3294-3296, Jul. 2019.

[17] B. S. Palmintier and M. D. Webster, "Heterogeneous unit clustering for efficient operational flexibility modeling," *IEEE Transactions on Power Systems*, vol. 29, no. 3, pp. 1089-1098, May 2014.

[18] J. Meus, K. Poncelet, and E. Delarue, "Applicability of a clustered unit commitment model in power system modeling," *IEEE Transactions on Power Systems*, vol. 33, no. 2, pp. 2195-2204, Mar. 2018.

[19] Y. Wei, Q. Zhai, P. Li *et al.*, "Fast solution method for TCUC with long time horizon based on horizon splitting," *International Journal of Electrical Power & Energy Systems*, vol. 112, pp. 61-69, Apr. 2019.

[20] F. Safdarian, A. Mohammadi, and A. Kargarian, "Temporal decomposition for security-constrained unit commitment," *IEEE Transactions on Power Systems*, vol. 35, no. 3, pp. 1834-1845, May 2020.

[21] Q. Zhai, X. Guan, J. Cheng *et al.*, "Fast identification of inactive security constraints in SCUC problems," *IEEE Transactions on Power Systems*, vol. 25, no. 4, pp. 1946-1954, Nov. 2010.

[22] J. Wang, J. Wei, Y. Zhu *et al.*, "The reliability and operational test system of a power grid with large-scale renewable integration," *CSEE Journal of Power and Energy Systems*, vol. 6, no. 3, pp. 704-711, Sept. 2020.

[23] I. Peña, C. B. Martinez-Anido, and B. Hodge, "An extended IEEE 118-bus test system with high renewable penetration," *IEEE Transactions on Power Systems*, vol. 33, no. 1, pp. 281-289, Jan. 2018.

Qian Yang received the B.S. degree in electrical engineering from North China Electric Power University, Baoding, China, in 2018, and is currently pursuing the Ph.D. degree in electrical engineering at Xi'an Jiaotong University, Xi'an, China. His research interests include power system operation and planning.

Jianxue Wang received the B.S., M.S., and Ph.D. degrees in electrical engineering from Xi'an Jiaotong University, Xi'an, China, in 1999, 2002, and 2006, respectively. He is currently a Professor in the School of Electrical Engineering, Xi'an Jiaotong University. His current research interests include power system operation and planning, microgrid operation and planning, and electricity market.

Hongrui Yin received the B.S. degree in electrical engineering from Chongqing University, Chongqing, China, in 2019, and is currently pursuing the M.S. degree in electrical engineering at Xi'an Jiaotong University, Xi'an, China. His research interests include power system operation and planning.

Qingtao Li received the B.S. degree in electrical engineering from Xi'an Jiaotong University, Xi'an, China, in 2016, where he is currently pursuing the Ph.D. degree. His research interests include generation expansion planning and scheduling, and market-based power system planning.